



<b>Publication Year</b>	2016
<b>Acceptance in OA</b>	2020-04-29T11:55:00Z
<b>Title</b>	Spectral optical constants of ethanol and isopropanol from ultraviolet to far infrared
<b>Authors</b>	Sani, Elisa, DELL'ORO, Aldo
<b>Publisher's version (DOI)</b>	10.1016/j.optmat.2016.06.041
<b>Handle</b>	<a href="http://hdl.handle.net/20.500.12386/24307">http://hdl.handle.net/20.500.12386/24307</a>
<b>Journal</b>	OPTICAL MATERIALS
<b>Volume</b>	60

( )

Paper published on: **Optical Materials** vol. **60** (2016) pages **137-141**; DOI: 10.1016/j.optmat.2016.06.041

**Numerical data associated with this paper can be found in the online version at** <http://dx.doi.org/10.1016/j.optmat.2015.06.039>

## Spectral optical constants of ethanol and isopropanol from ultraviolet to far infrared

Elisa Sani<sup>a,1</sup>, Aldo Dell'Oro<sup>b</sup>

<sup>a</sup>*INO-CNR, Istituto Nazionale di Ottica, largo E. Fermi, 6, 50125 Firenze (Italy)*

<sup>b</sup>*INAF Osservatorio Astrofisico di Arcetri, largo E. Fermi, 5, 50125 Firenze (Italy)*

---

### Abstract

Ethanol and isopropanol are fluids of common use in different branches of materials science. In particular, in the ever growing field of nanoscience, they are dispersing media for nanoparticle suspensions. The knowledge of optical constants of these fluids is required for the characterization of optical properties of nanoparticles, besides providing insights into fundamental properties of fluids themselves. In this work, we calculated the real refractive index  $n$  of ethanol and isopropanol applying the Kramers-Kronig theory to the experimentally obtained  $k$  spectrum over an extremely wide spectral range, from 181 to  $\sim 54000$   $\text{cm}^{-1}$ .

*Keywords:* Optical constants, Optical properties, Liquid phase, Ethanol, Isopropanol, Nanofluids

---

### 1. Introduction

Nanotechnologies are impressively fast growing. Nanofluids (i.e. fluids with nanosized particles in suspension) are correspondingly receiving an always increasing attention and are considered promising in a large variety of

---

<sup>1</sup>Corresponding author, email: elisa.sani@ino.it

applications. Even if ions to control pH or surfactants can be added to improve stability, the two main ingredients of a nanofluid remain nanoparticles and base fluid. Nanofluids are expected, and in many cases proved, to show superior properties with respect to the pure fluid for many applications like for instance in thermal, optical or tribological fields [1]-[4]. Nanofluid properties can be controlled and tuned by the proper combination of nanoparticles and dispersing liquid. Nanoparticles can now be produced in a huge variety of materials, sizes and shapes, and new types are ever synthesized. The investigation of their optical properties is an important tool to understand their basic physics, as well as to assess their potential in all application fields requiring interaction with optical radiation. However, according to the Mie theory [5] optical properties of nanoparticles are influenced by those of the dispersing medium [6], so that their dependence as a function of the surrounding refractive index is an important characteristics widely investigated in the literature [7]-[10].

Ethanol and isopropanol (2-propanol) are common dispersing media for nanoparticle suspensions and are used also by commercial suppliers of nanocolloids. Their refractive index and absorption coefficient are typically known in limited spectral ranges or even at the single wavelength of the sodium D-line [11]-[18]. However, new nanoparticles are recently raising the attention, with exotic absorption peaks spanning from visible to near-infrared wavelengths [19]-[21]. The knowledge of optical constants of the fluid surrounding these new kinds of nanomaterials is needed for different applications like for instance for modelling optical properties and radiative transfer. For this reason, in the present work we considerably extend the wavelength range of knowledge of  $(k,n)$  optical constants of ethanol and isopropanol. This work is a part of a project aimed at obtaining optical constants of a significant number of fluids used in nanoparticle synthesis and characterization. The optical constant  $k$  is experimentally obtained from 0.185  $\mu\text{m}$  to about 55  $\mu\text{m}$  ( $\sim 54000\text{-}181\text{ cm}^{-1}$ ) from transmittance measurements. Then, the refractive index  $n$  is obtained from experimental  $k$  spectrum by means of the Kramers-Kronig transform. It is worthwhile to note that the extremely wide wavelength range we have explored allows the use of the Kramers-Kronig transform technique, avoiding truncation errors over most of the spectral range. At the bounds of the interval, a special treatment is required, as discussed below.

## 2. Experimental setup

The optical transmittance spectra of ethanol (J.T. Baker, purity  $\geq 99.9\%$ ) and isopropanol (Merck, purity  $\geq 99.8\%$ ) have been measured by means of three different experimental setups: a "Lambda 900" Perkin-Elmer dispersive spectrophotometer for the range  $\sim 54054\sim 33333\text{ cm}^{-1}$  ( $0.185\sim 3\text{ }\mu\text{m}$ ), a Fourier transform "Excalibur" Bio-Rad spectrometer with KBr optics for the wavenumber range  $5500\sim 400\text{ cm}^{-1}$  ( $\sim 1.8\sim 25\text{ }\mu\text{m}$ ) and finally a Fourier transform "Scimitar" Bio-Rad spectrometer with polyethylene windows and mylar beam splitter for the range  $420\sim 181\text{ cm}^{-1}$  ( $\sim 24\sim 55\text{ }\mu\text{m}$ ). The combination of these three instruments allows to span a spectral interval as wide as from  $\sim 54000$  ( $0.185\text{ }\mu\text{m}$ ) to  $181\text{ cm}^{-1}$  ( $\sim 55\text{ }\mu\text{m}$ ). Except when differently specified, the transmittance has been measured at different sample thicknesses using a demountable variable-path cell composed by two optical windows and by a series of calibrated spacers with  $50\sim 1130\text{ }\mu\text{m}$  thickness. When the sample transmittance was too low to have a detectable signal at the output (like in mid- and far-infrared), we assembled the cell without spacer as described in the following. On the contrary, when the transmittance of fluids was very high (e.g. in the visible range), arising in very low  $k$  values with high relative uncertainty, we used a specially designed demountable cell with 5, 8, 10 and 12.5 mm path length. The materials we have chosen for cell windows in the different spectral regions have been  $\text{CaF}_2$  for the  $0.185\sim 3.00\text{ }\mu\text{m}$  range, with exception of the interval  $0.25\sim 1.40\text{ }\mu\text{m}$ , where fused silica was used (long path cell for reducing the relative uncertainty on  $k$ , as explained above); KBr for  $\sim 1.8\sim 25\text{ }\mu\text{m}$  and polyethylene for  $\sim 24\sim 55\text{ }\mu\text{m}$ .

## 3. Transmittance measurements

We obtained the spectral optical constant  $k$  from transmittance measurements using the technique described in [24] and here recalled for clarity.

Under the hypotheses of absence of scattering, negligible coherent effects [5] and negligible multiple transmissions through the sample, the transmittance  $T$  as a function of the wavenumber  $\nu$  can be expressed as a simple function of the spectral absorption coefficient  $\alpha(\nu)$  as

$$T(\nu) = \exp(-\alpha(\nu) \cdot x) \quad (1)$$

where  $x$  indicates the sample thickness. Therefore, if we acquire two transmittance spectra  $T_1$  and  $T_2$  at two different thicknesses  $x_1$  and  $x_2$ ,  $\alpha$  can be

obtained from the equation:

$$\alpha(\nu) = -\frac{1}{x_2 - x_1} \ln \frac{T_2(\nu)}{T_1(\nu)} = -\frac{1}{\Delta x} \ln \frac{T_2(\nu)}{T_1(\nu)} \quad (2)$$

This simple method allows to directly obtain  $\alpha$  for the liquid sample without requirement of a prior knowledge of optical properties (complex refractive index) of window materials and without the need of using complex equations like those arising from the three-layer system approach. The spectral optical constant  $k(\nu)$ , i.e. the imaginary part of the complex refractive index, is connected to  $\alpha(\nu)$  by the relationship [5]:

$$k = \frac{\alpha(\nu)}{4\pi\nu} \quad (3)$$

In the range 0.185-3.00  $\mu\text{m}$  (UV-Vis-NIR) we acquired the transmittance spectra at several cell thicknesses from 50 to 1130  $\mu\text{m}$ , and we kept as  $\alpha$  to be used in further calculations the value obtained by averaging the result of Eq. 2 for several couples of thicknesses ( $x_1$ ,  $x_2$ ). Moreover, as explained above, in the spectral range from about 0.25  $\mu\text{m}$  to 1.40  $\mu\text{m}$  wavelength, additional transmittance measurements were carried out to reduce the uncertainty on  $k$  using a special cell allowing much longer millimetric path lengths, from 5 to 12.5 mm. The spectral resolution is  $1 \times 10^{-3}$   $\mu\text{m}$  in the range 0.185-0.860  $\mu\text{m}$  and varies from  $3 \times 10^{-3}$  to  $2 \times 10^{-2}$   $\mu\text{m}$  at longer wavelengths. The relative uncertainty of transmittance values is 0.5%.

In Mid-Infrared (MIR) (5500-400  $\text{cm}^{-1}$  wavenumbers,  $\sim 1.8\text{-}\sim 25$   $\mu\text{m}$  wavelength) and Far-Infrared (FIR) (420-181  $\text{cm}^{-1}$ ,  $\sim 24\text{-}\sim 55$   $\mu\text{m}$ ) ranges, the transmittance was zero or near to it in a large majority of the spectrum even with the thinnest 50  $\mu\text{m}$  spacer because of strong absorption bands due to molecular stretching and bending modes [22]-[23]. Thus, we used the method without spacer we successfully exploited in our previous work [24] and firstly presented in [25]. The absence of the spacer in the cell allows to obtain very thin layers of liquid. Their (unknown) thickness can be changed acting on the tightening levels of the cell nuts. For the determination of  $\alpha$ , Eq. 2 requires only the knowledge of the difference of thickness  $\Delta x$  among two measurements, which was inferred as follows: MIR region, for each considered couple of measurements,  $\Delta x$  was chosen to match, in the regions of spectral superposition of the Mid-IR and UV-Vis-NIR instruments, the value of  $\alpha$  previously determined by the UV-Vis-NIR measurements; in the FIR,  $\Delta x$

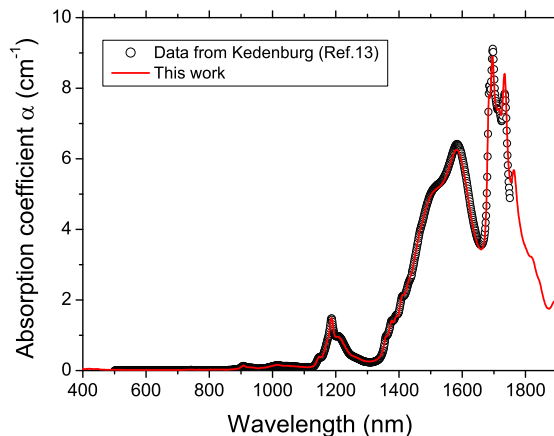


Figure 1: Comparison between measured and literature data [13] for ethanol in the visible-near infrared.

was similarly determined imposing equality of FIR  $\alpha$  spectrum to previously determined MIR values, again in the region of spectral superposition of MIR and FIR instruments. The spectral resolution of NIR and FIR measurements is  $1 \text{ cm}^{-1}$ . The relative uncertainty on transmittance is between 0.05% and 0.3% depending on the spectral region.

The shape of acquired transmittance curves in MIR for both liquids agree with qualitative spectra available in the literature [22], [23]. As for quantitative data, Fig. 1 compares the absorption coefficient for ethanol in the visible-near infrared measured in this work with the only available literature data [13], showing a fair agreement.

Once  $\alpha(\nu)$  was obtained as described, the optical constant  $k(\nu)$  was calculated from Eq. 3. The experimental values of  $k(\nu)$  for ethanol and isopropanol are shown in red color in Figures 2 and 3, respectively. While the detailed interpretation of the intricate structure of absorption bands is by far beyond the scope of the present work and can be found in molecular spectroscopy literature [26]-[27], looking at the plots (a) and (b) of Figs. 2-3, we can recognize the typical vibrational bands of functional groups of alcohols [26], e.g. the wide OH stretching band at around  $3300\text{-}3400 \text{ cm}^{-1}$ , CH stretching at around  $3000 \text{ cm}^{-1}$  and CO stretching in the  $1050\text{-}1200 \text{ cm}^{-1}$  region.

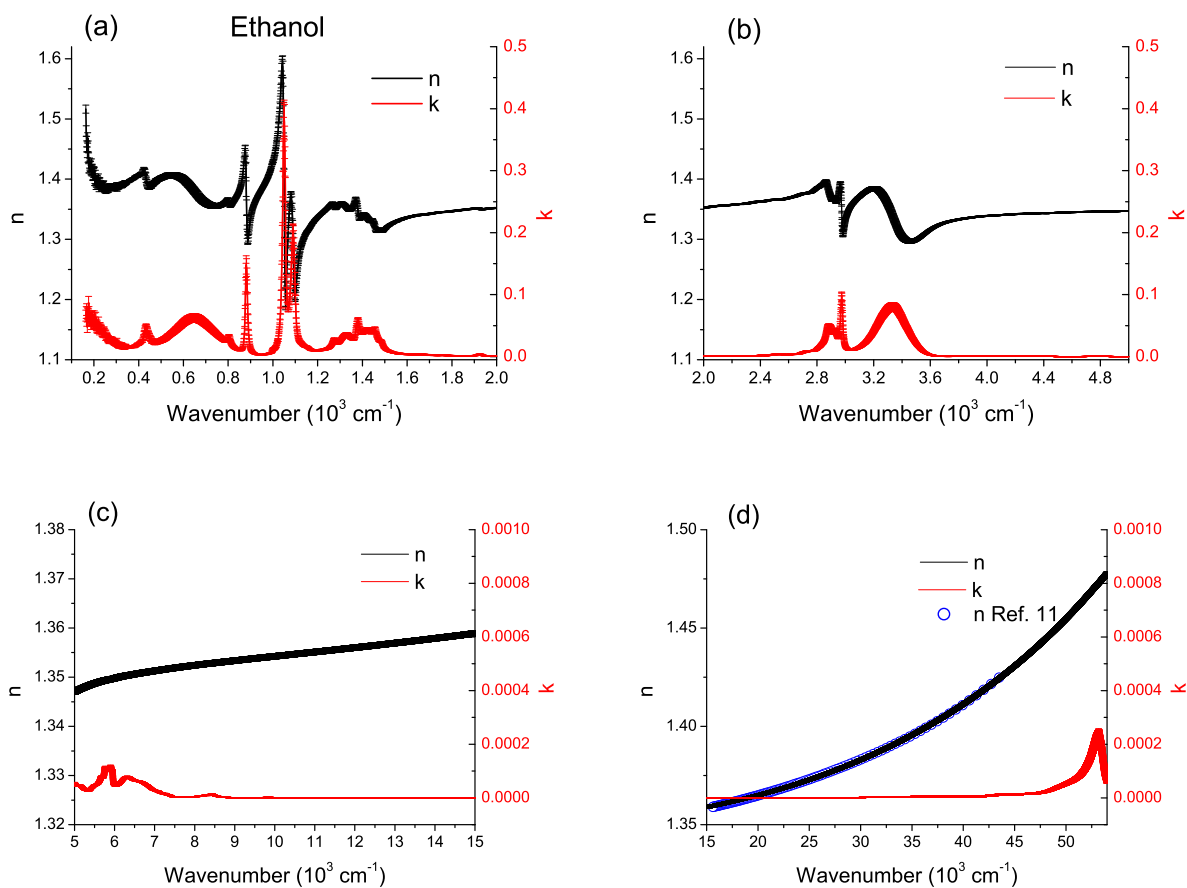


Figure 2: Optical constants  $n$  (in black, left axis) and  $k$  (in red, right axis) for ethanol. In (d)  $n$  data from [11] are also plotted as blue circles, with exaggerated size to make them visible. Actually they lie within our uncertainty on  $n$ .

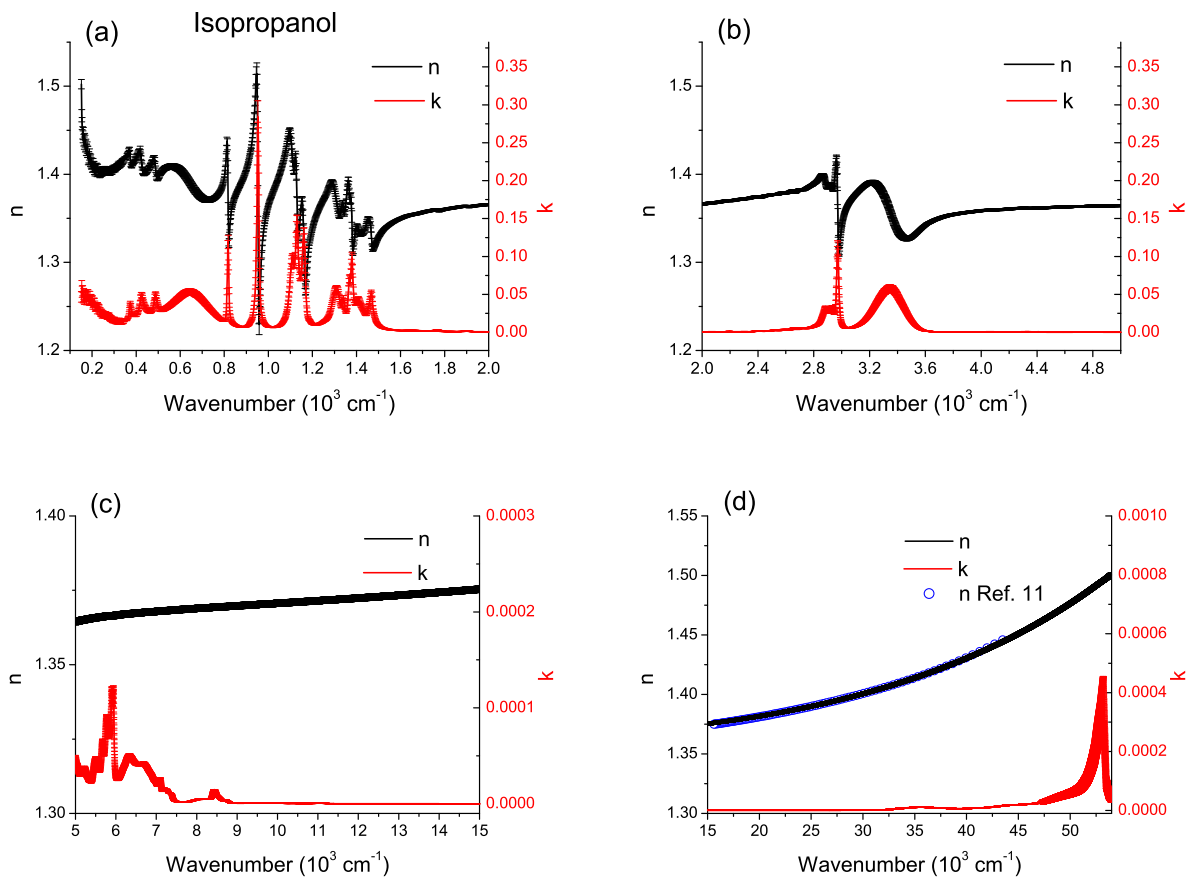


Figure 3: Optical constants  $n$  (in black, left axis) and  $k$  (in red, right axis) for isopropanol. In (d)  $n$  data from [11] are also plotted as blue circles, with exaggerated size to make them visible. Actually they lie within our uncertainty on  $n$ .

#### 4. Refractive index

The refractive index  $n(\nu)$  and the  $k(\nu)$  optical constant represent, respectively, the real and imaginary part of the complex refractive index  $m(\nu) = n(\nu) + ik(\nu)$ . Thus they are related each other through the Kramers-Kronig relationship, which can be used to calculate  $n(\nu)$  from the experimental  $k(\nu)$  spectrum:

$$n(\nu) = n(\infty) + \frac{2}{\pi} P \int_0^{\infty} \frac{\nu' k(\nu')}{\nu'^2 - \nu^2} d\nu' \quad (4)$$

where  $P$  identifies the Cauchy's principal part of the integral and  $n(\infty)$  is the value of the refractive index at high wavenumbers. The integral in Eq. 4 has been numerically computed using the Maclaurin's formula [28]. The uncertainty on  $n(\nu)$  has been calculated propagating the experimental uncertainty on  $k(\nu)$ . As for the constant value  $n(\infty)$  in Eq. 4, it is not known. Generally it is indirectly obtained imposing a known value of  $n$  at a given wavenumber.

The major technical limitation of the method based on the Kramers-Kronig transform is that the integral in Eq. 4 should be calculated from zero to infinity and different approaches have been discussed in the literature to overcome this issue [29]-[31]. Even if this requirement is not experimentally possible,  $n(\nu)$  can be computed with a satisfactory accuracy if  $k$  is known in an enough wide interval of wavenumbers around  $\nu$ . Truncation errors can occur near the boundaries of the spectral interval of known  $k$ , depending on the (unknown) values of  $k$  outside the range available for experimental exploration [29]. As discussed in [24], at the low-energy side (low wavenumbers), in a conservative way we can estimate that, for  $\nu$  larger than 300/400  $\text{cm}^{-1}$ , the error  $\Delta n$  due to the truncation of the integral in Eq. 4 is comparable or smaller than the uncertainty of  $n$  due to the measurement errors. On the other hand, at high wavenumbers (short wavelengths) a clear effect of truncation appears. In fact, if we apply the Kramers-Kronig algorithm without the extrapolation described below, i.e. if we use only the data of  $k$  in the available experimental range, the computed values of  $n$  in the visible-near infrared should result to be roughly independent on  $\nu$  while from literature we know that in the same range  $n$  increases with wavenumber [11]- [13]. This behavior of  $n$  is compatible with the increasing phase of the refractive index near to a region of anomalous dispersion, corresponding to a peak of  $k$ . Following the method already successfully exploited for ethylene glycol

[24], for each fluid we best-fitted, with a lorentzian peak in  $k$ , the literature values of  $n$  given in [11]. For both liquids, the best solution consists of a peak around  $\sim 100000 \text{ cm}^{-1}$  (and exactly located at  $97991 \text{ cm}^{-1}$  and  $96854 \text{ cm}^{-1}$  for ethanol and isopropanol, respectively), which provides a negligibly small value of  $k$  in the range of interest. However, this main peak is not able to reproduce the increasing trend of the  $k$  curve at the upper energy boundary of the experimentally available range. Thus, to check the validity of our model, for diagnostic purposes we ascertained that the experimental  $k$  curve in the range  $54000\text{-}41600 \text{ cm}^{-1}$  could be correctly reproduced by lorentzian oscillators, and we analyzed how they impact on the known values of  $n$ . The  $k$  spectrum was thus fitted with the minimum number of Lorentz oscillators able to satisfactorily reproduce the experimental trend (secondary oscillators). We verified that only the main peak set the value of  $n$ , while (much smaller) secondary oscillators introduce variations on it much smaller than the experimental uncertainty. It should be stressed that the  $k$  fitting with secondary peaks has been performed only to guarantee the continuity of the  $k$  function within the extrapolation of the main oscillator we carried out using the Lorentz theory. Differently on the main peak, they have not been used in the calculation of Eq. 4, because they all refer to a spectral region where experimental data are available. In summary, main and secondary peaks together are able to fairly reproduce both  $n$  and  $k$  in the range  $15000\text{-}41600 \text{ cm}^{-1}$ . Thus, the described extrapolation of the  $k$  spectrum is able to correct the truncation error of the Kramers-Kronig transform at high wavenumbers and allows the correct determination of the zero point  $n(\infty)$ .

Finally, for operating purposes it can be useful to give an analytical expression for  $n$  when possible. Thus we fitted the obtained refractive indexes of both liquids with a four-parameter Sellmeier equation [32], using a least-squares algorithm:

$$n^2 = 1 + \frac{B \cdot \lambda^2}{\lambda^2 - C} + \frac{D \cdot \lambda^2}{\lambda^2 - E} \quad (5)$$

We emphasize that this approach is intrinsically limited to spectral regions without absorption bands, because, in the vicinity of absorption peaks (corresponding to the zeros of denominators in Eq. 5), Sellmeier polynomials give the physically unacceptable result of diverging  $n$  values. Table 1 lists the obtained parameters for ethanol and isopropanol in the range  $0.185\text{-}2.800 \mu\text{m}$ .

Parameter	Ethanol	Isopropanol
B	0.0165±0.0002	0.0107±0.0003
C	9.08±0.02	8.88±0.03
D	0.8268±0.0001	0.8702±0.0002
E	0.01039±0.00001	0.01036±0.00002

Table 1: Sellmeier parameters (Eq. 5) for the investigated liquids in the spectral range from 0.185 to 2.800  $\mu\text{m}$ .

## 5. Conclusions

In this work we have obtained the real and imaginary parts,  $n$  and  $k$ , of the complex refractive index of ethanol and isopropanol over an extremely wide spectral range.  $k$  is experimentally obtained from transmittance measurements, while  $n$  is calculated from  $k$  thanks to the very large spectral range of available experimental data, using the Kramers-Kronig theory, corrected with an *ad-hoc* technique of extrapolation to avoid truncation errors at the edges of the experimental spectrum. For application purposes, Sellmeier parameters are also given in the range 0.185-2.800  $\mu\text{m}$ .

## Acknowledgements

Authors gratefully acknowledge Mr. Massimo D'Uva of INO mechanical workshop and Mr. Mauro Pucci of INO optical workshop for technical assistance. A part of this activity has been carried out within the framework of the SOLE-2 project funded by the Italian bank foundation Ente Cassa di Risparmio di Firenze (pratica n. 2014.0711).

## References

## References

- [1] Z. Said, M.H. Sajid, R. Saidur, M. Kamalifarvestani, N.A. Rahim, Radiative properties of nanofluids, *International Communications in Heat and Mass Transfer*, 46 (2013)74-84

Paper published on:

**Optical Materials vol. 60 (2016) pages 137-141**

DOI: 10.1016/j.optmat.2016.06.041

**Numerical data associated with this paper can be found in the  
online version at**

<http://dx.doi.org/10.1016/j.optmat.2015.06.039>

---

- [2] R. Saidur, K.Y. Leong, H.A. Mohammad, A review on applications and challenges of nanofluids, *Renewable and Sustainable Energy Reviews*, 15 (2011) 1646-1668
- [3] L. Godson, B. Raja, D. Mohan Lal, S. Wongwises, Enhancement of heat transfer using nanofluids - An overview, *Renewable and Sustainable Energy Reviews*, 14 (2010) 629-641
- [4] V. Eswaraiah, V. Sankaranarayanan, S. Ramaprabhu, Graphene-Based Engine Oil Nanofluids for Tribological Applications *ACS Applied Materials & Interfaces* 3 (2011), 4221-4227
- [5] C. F. Bohren, D. R. Huffman, 2004 *Absorption and Scattering of Light by Small Particles.*, Wiley
- [6] F. Cocchini, F. Bassani, M. Bourg, Model calculation of the optical properties of metallic particles in a dielectric medium, *Surface Science* 156 (1985) 851-858
- [7] N. G. Khlebtsov, L. A. Trachuk, A. G. Melnikov, The Effect of the Size, Shape, and Structure of Metal Nanoparticles on the Dependence of Their Optical Properties on the Refractive Index of a Disperse Medium, *Opt. Spectr.* 98 (2005) 77-83.
- [8] Y. Sun, Y. Xia, Gold and silver nanoparticles: A class of chromophores with colors tunable in the range from 400 to 750 nm, *Analyst* 128 (2003) 686-691
- [9] M. A. Mahmoud, M. A. El-Sayed, Gold Nanoframes: Very High Surface Plasmon Fields and Excellent Near-Infrared Sensors, *J. American Chemical Society* 132 (2010) 12704-12710
- [10] M. M. Miller, A. A. Lazarides, Sensitivity of Metal Nanoparticle Surface Plasmon Resonance to the Dielectric Environment, *J. Physical Chemistry B* 109 (2005) 21556-21565
- [11] I. Z. Kozma, P. Krok, and E. Riedle. Direct measurement of the group-velocity mismatch and derivation of the refractive-index dispersion for a variety of solvents in the ultraviolet, *J. Opt. Soc. Am. B* 22, 1479-1485 (2005)

Paper published on:  
**Optical Materials vol. 60 (2016) pages 137-141**  
DOI: 10.1016/j.optmat.2016.06.041  
**Numerical data associated with this paper can be found in the  
online version at**  
<http://dx.doi.org/10.1016/j.optmat.2015.06.039>

---

- [12] J. Rheims, J Kser and T Wriedt. Refractive-index measurements in the near-IR using an Abbe refractometer, *Meas. Sci. Technol.* 8, 601-605 (1997)
- [13] S. Kedenburg, M. Vieweg, T. Gissibl, and H. Giessen. Linear refractive index and absorption measurements of nonlinear optical liquids in the visible and near-infrared spectral region, *Opt. Mat. Express* 2, 1588-1611 (2012)
- [14] Scott T.A. Jr, Refractive index of ethanol-water mixtures and density and refractive index of ethanol-water-ethyl ether mixtures, *J Phys Chem.* 50 (1946) 406-12
- [15] Physical behavior of some reaction media. Density, viscosity, dielectric constant, and refractive index changes of ethanol-cyclohexane mixtures at several temperatures Georgios E. Papanastasiou and Ioannis I. Ziogas *Journal of Chemical and Engineering Data* 1991 36 (1), 46-51
- [16] L. Albuquerque, C. Ventura, R. Goncalves, "Refractive Indices, Densities, and Excess Properties for Binary Mixtures Containing Methanol, Ethanol, 1,2-Ethanediol, and 2-Methoxyethanol", *J. Chem. Eng. Data* 41 (1996) 685-688
- [17] J. V. Herraez, R. Belda, Refractive Indices, Densities and Excess Molar Volumes of Monoalcohols + Water, *J. Solution Chemistry* 35 (2006) 1315-1328
- [18] Kwang-Yu Chu and A. R. Thompson, Densities and Refractive Indices of Alcohol-Water Solutions of n-Propyl, Isopropyl, and Methyl Alcohols, *J. Chemical and Engineering Data* 7 (1962) 358-360
- [19] S. J. Oldenburg, J. B. Jackson, S. L. Westcott, N. J. Halas, Infrared extinction properties of gold nanoshells, *Applied Physics Letters*, 75 (1999) 2897-2899
- [20] R. Bukasov, J. S. Shumaker-Parry, Highly Tunable Infrared Extinction Properties of Gold Nanocrescents, *Nano Letters* 7 (2007) 1113-1118
- [21] D. Dorfs et al, Reversible Tunability of the Near-Infrared Valence Band Plasmon Resonance in  $\text{Cu}_{2-x}\text{Se}$  Nanocrystals, *Journal of the American Chemical Society* 133 (2011) 11175-11180

Paper published on:  
**Optical Materials vol. 60 (2016) pages 137-141**  
DOI: 10.1016/j.optmat.2016.06.041  
**Numerical data associated with this paper can be found in the  
online version at**  
<http://dx.doi.org/10.1016/j.optmat.2015.06.039>

---

- [22] Infrared spectrum of isopropyl alcohol from NIST database <http://webbook.nist.gov/cgi/cbook.cgi?ID=C67630&Type=IR-SPEC&Index=3>
- [23] Infrared spectrum of ethyl alcohol from NIST database <http://webbook.nist.gov/cgi/cbook.cgi?ID=C64175&Type=IR-SPEC&Index=3>
- [24] E. Sani, A. Dell’Oro, Optical constants of ethylene glycol over an extremely wide spectral range, *Optical Materials* 37 (2014) 36-41
- [25] A. Barbaro, G. Cecchi, P. Mazzinghi, Oil UV extinction coefficient measurement using a standard spectrophotometer, *Applied Optics* 30 (1991)852-857
- [26] E. K. Plyler, Infrared Spectra of Methanol, Ethanol, and n-Propanol, *J. Research National Bureau of Standards* 48 (1952) 281-286
- [27] G. Herzberg, *Infrared and Raman spectra of polyatomic molecules* (D. Van Nostrand Co, Inc., New York 1945)
- [28] Ohta K. Ishida H., ”Comparison Among Several Numerical Integration Methods for Kramers-Kronig Transformation”, *Applied Spectroscopy*, Vol 42 (1988), 952-957.
- [29] J. P. Hawranek, R. N. Jones, ”The control of errors in i.r. spectrophotometry-V. Assessment of errors in the evaluation of optical constants by transmission measurements on thin films”, *Spectrochimica Acta*, Vol. 32A (1976) 99-109
- [30] D. M. Roessler, ”Kramers - Kronig analysis of reflectance data: III. Approximations, with reference to sodium iodide”, *Br. J. Appl. Phys.* 17 (1966) 1313 doi:10.1088/0508-3443/17/10/309
- [31] K. F. Palmer, M. Z. Williams, B. A. Budde, ”Multiply subtractive KramersKronig analysis of optical data”, *Applied Optics*, Vol. 37, (1998) 2660-2673
- [32] W. Sellmeier, ”Zur Erklärung der abnormen Farbenfolge im Spectrum einiger Substanzen”, *Ann. Phys. Chem.* 143, 271 (1871)